



**HAL**  
open science

## **A new experimental methodology to assess gear scuffing initiation**

Nicolas Grenet de Bechillon, Thomas Touret, Jérôme Cavoret, Christophe Changenet, Fabrice Ville, Dhafer Ghribi

► **To cite this version:**

Nicolas Grenet de Bechillon, Thomas Touret, Jérôme Cavoret, Christophe Changenet, Fabrice Ville, et al.. A new experimental methodology to assess gear scuffing initiation. Tribology - Materials, Surfaces & Interfaces, 2022, 16 (3), pp.245-255. 10.1080/17515831.2022.2045427 . hal-04176212

**HAL Id: hal-04176212**

**<https://hal.science/hal-04176212v1>**

Submitted on 2 Aug 2023

**HAL** is a multi-disciplinary open access archive for the deposit and dissemination of scientific research documents, whether they are published or not. The documents may come from teaching and research institutions in France or abroad, or from public or private research centers.

L'archive ouverte pluridisciplinaire **HAL**, est destinée au dépôt et à la diffusion de documents scientifiques de niveau recherche, publiés ou non, émanant des établissements d'enseignement et de recherche français ou étrangers, des laboratoires publics ou privés.

# A new experimental methodology to assess gear scuffing initiation

Nicolas GRENET -- de BECHILLON<sup>a,b,c</sup>  
nicolas.grenet--debechillon@insa-lyon.fr

Thomas TOURET<sup>b</sup>  
thomas.touret@ecam.fr

Jérôme CAVORET<sup>a</sup>  
jerome.cavoret@insa-lyon.fr

Christophe CHANGENET<sup>b</sup>  
christophe.changenet@ecam.fr

Fabrice VILLE<sup>a</sup>  
fabrice.ville@insa-lyon.fr

Dhafer GHRIBI<sup>c</sup>  
dhafer.ghribi@safrangroup.com

<sup>a</sup>Univ Lyon, INSA Lyon, CNRS, LaMCoS, UMR5259, 69621 Villeurbanne, France

<sup>b</sup>Univ Lyon, ECAM LaSalle, LabECAM, 69321 Lyon, France

<sup>c</sup>Safran Transmission Systems, 92700 Colombes, France

Corresponding author: fabrice.ville@insa-lyon.fr

## Abstract

This paper investigates the strong coupling between friction power losses and film thickness that prevent from clearly identifying the mechanism of scuffing through classical test procedures. As the film thickness appears of great influence on the phenomena, a new test method is presented allowing scuffing **initiation** study with the film thickness as a key parameter. This new test method allows film thickness variation with minimal friction losses and bulk temperature variations. **This procedure has been developed with nitrided steels and a synthetic base oil on a twin disks test rig.** Even though asperity contact is considered necessary in literature for scuffing, test result shows that it can be reached in full film lubrication, potentially through the collapse of the oil film. Different test methods allowing triggering scuffing through different parameters are identified, **which shows that a variety of parameters is able to influence scuffing.**

Keywords: gear scuffing, twin disks, oil film thickness, bulk temperature, friction losses

## 1 Introduction

2 Gear scuffing is commonly defined by localized welding of contacting surfaces with material transfer  
3 under severe operating conditions [1]. This subject has been widely studied, as it is a sudden  
4 destructive failure that may lead to the ruin of a mechanical transmission. Several reviews on this topic  
5 can be cited like Dyson [1][2], Grosberg [3], Bowman and Stachowiak [4], Ludema [5] or Castro and  
6 Seabra [6]. From the literature, two main approaches can be identified: power-based and oil film-  
7 based.

8  
9 A first trend was based on the hypothesis that scuffing occurs once a critical friction power loss is  
10 reached in the contact. The main first attempt to explain scuffing is given by Almen [7]–[9] with the  
11 pressure times sliding velocity (PV) criterion. Two major criteria were built on this base and  
12 accounting for the friction coefficient: the Friction Power Intensity (FPI) and Friction Power (FP) by  
13 Matveevsky [10], [11]. These concepts were later adapted to thermal considerations with the flash  
14 temperature for line contact by Blok [12], [13], and for elliptical contact by Muzychka and  
15 Yovanovich [14] with the estimation of the instantaneous and localized temperature rise occurring in a  
16 fully lubricated contact. This last criterion highlights the importance of the bulk temperature for  
17 scuffing understanding.

18  
19 As most of gears operate under mixed lubrication regime, another main approach to analyze scuffing  
20 is based on the concept that asperity contact is necessary for scuffing initiation, hence the question of  
21 the lubrication regime. Scuffing may occur when the lubricant film thickness is insufficient to provide  
22 suitable separation of the contacting surfaces, either when the operating conditions do not allow for  
23 sufficient film or by its breakdown [15].

24 The reduced film thickness defined by Tallian [16], [17] generally used to define the lubrication  
25 regimes has been used as a scuffing criteria [1], [6], [18]. This parameter compares the minimal film  
26 thickness to the roughness of the surfaces.

27  
28 To investigate gear scuffing, most studies include experimentations performed on different test rigs  
29 such as four-ball [19], [20], ball on disk [21], [22], twin disks [23]–[25] or back-to-back gear test rigs  
30 [6], [18], [26], [27]. As knowledge on this failure develops and grows, a number of parameters  
31 influencing gear scuffing can be listed:

- 32 • normal load, contact pressure,
- 33 • sliding and entrainment speeds,
- 34 • surface roughness and finish,
- 35 • hardness and material properties,
- 36 • lubricant type, viscosity, additives, flow rate,
- 37 • bulk temperature,
- 38 • friction coefficient, etc.

39 As the mechanism of scuffing is not fully understood, further work through a physics based approach  
40 is required. In a first part, this paper presents the physical mechanisms at work during commonly used  
41 test procedures for scuffing investigation and identify the strong coupling between parameters. In a  
42 second part, a new test method allowing isolating the influence of film thickness on scuffing **initiation**  
43 is presented. As scuffing seems to be achievable through different parameters, an additional test  
44 highlighting the importance of bulk temperature is introduced. Finally, the complexity of this type of  
45 failure is discussed.

## 1 Traction tests

2 Most test procedures in literature aim to voluntarily increase the dissipated power through the normal  
 3 load and/or the sliding speed either gradually or continuously until scuffing occurs [23], [25], [28].  
 4 During this type of procedure, friction losses  $Q$  (see equation below) are driven up by the increase of  
 5 either load or sliding speed.

$$Q = \mu F_n v_s \quad (1)$$

6 Where  $F_n$  is the normal load,  $\mu$  is the friction coefficient and  $v_s$  is the sliding speed.

7 This dissipated power in the contact will result in heat flow through the material inducing temperature  
 8 rise. Such link between dissipated power and temperature in mechanical transmissions can be  
 9 observed during back-to-back gear tests where the augmentation of the load stage induces higher bulk  
 10 temperatures and hence oil bath temperatures [6] (Figure 1).

11

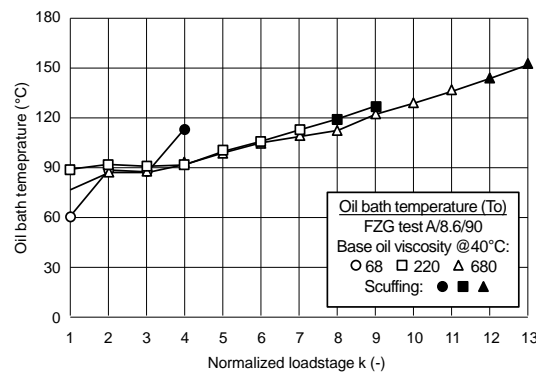


Figure 1: Evolution of the oil bath temperature with the applied load  $k$  (FZG stage), from [6]

12

13 The same coupling can be observed on various test rigs such as twin disks machine or ball on disk,  
 14 over different test methods. A common test procedure among them is the traction test. This procedure  
 15 consists in keeping the normal load, oil injection temperature and mean velocity at constant values  
 16 while the sliding speed is increased continuously until scuffing occurs or a predefined Slide-to-Roll  
 17 Ratio (SRR) is reached.

18

19 Following this method, Isaac *et al.* [23] performed scuffing tests on disks with transverse roughness  
 20 ( $R_a \approx 0.4 \mu\text{m}$ ) representative of a gear application with a MIL-L-699-PRF type lubricant (containing  
 21 additives). The test rig used was composed of two independently driven motors with one of them  
 22 being free in translation allowing the application of the intended load on the disks (Figure 2). This test  
 23 rig allows for friction measurements under controlled operating conditions and has been adapted for  
 24 bulk temperature measurements. Detailed descriptions of the test rig can be found in [29] and [23].

25

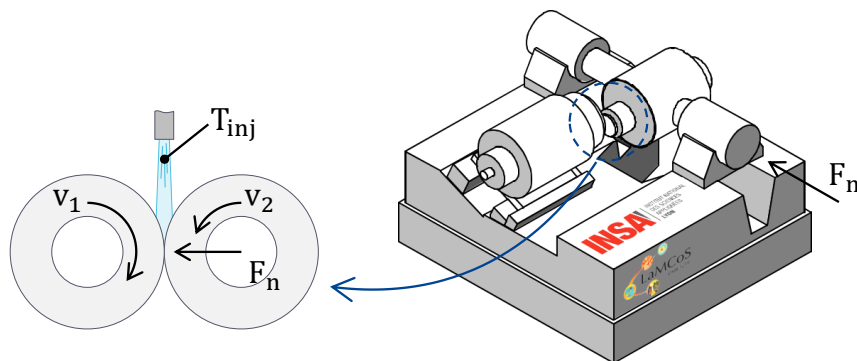


Figure 2: Presentation of the test rig

26

1 Three experiments from [23] are presented on Figure 3. All tests were performed at a maximum Hertz  
 2 contact pressure  $p_0$  of 1.6 GPa and an entrainment speed  $v_e=v_r/2=(v_1+v_2)/2$  of 21.9 m/s.  
 3

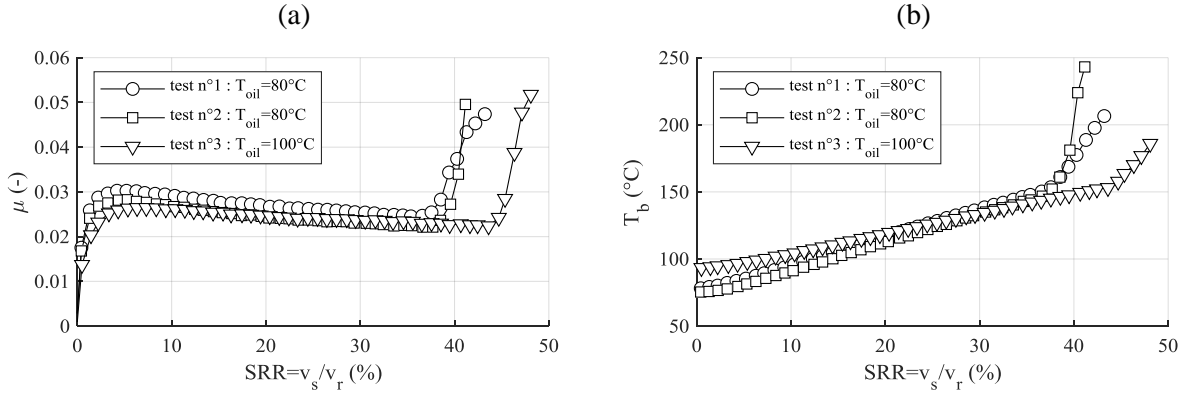


Figure 3: (a) Friction coefficient and (b) bulk temperatures obtained with rough surfaces, from [23]

4  
 5 The first two tests, performed in the same conditions for repeatability, scuffed at similar SRR value  
 6 ( $\approx 37\%$ ). The third test performed with higher injection temperature scuffed at higher SRR ( $\approx 44\%$ ).  
 7 Detailed analysis can be found in [23].

8 For all tests, the continuous increase in sliding directly affects the friction losses  $Q$  (equation (1))  
 9 (Figure 4a). This power is heat dissipated and, as a consequence, increases the disk bulk temperature  
 10 (Figure 3b) and reduces the oil film thickness  $h_m$  according to the model from Hamrock and Dowson  
 11 [30], [31] (Figure 4b). Those tests scuffed at similar levels of both friction losses and reduced film  
 12 thickness  $\Lambda=h_m/\sigma$ , highlighting the difficulty to determine which phenomena initiated scuffing.  
 13

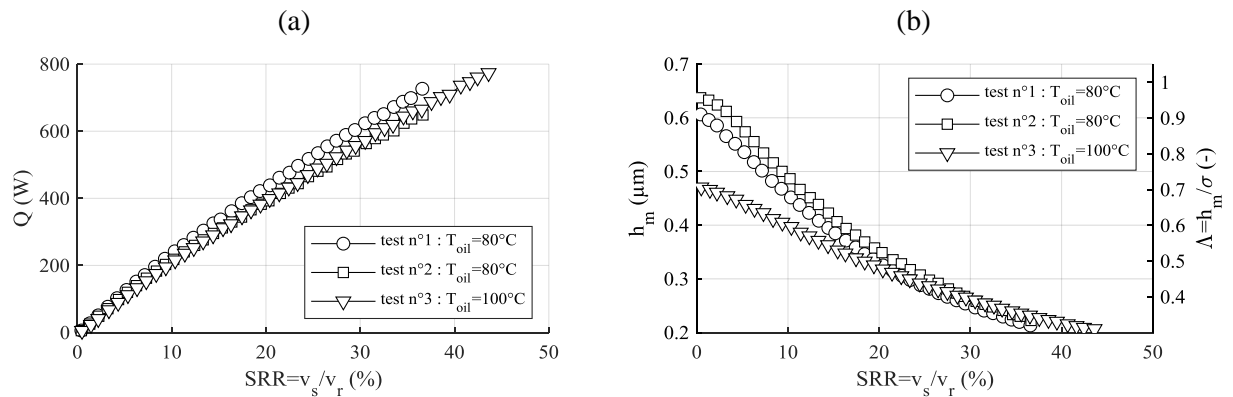


Figure 4: (a) Friction losses and (b) central film thickness evolution during the tests

14  
 15 When using a test method based on the increase of the friction power losses (such as traction tests or  
 16 load stages) the following phenomena occurs: as (i) the power loss in the contact increases instantly,  
 17 (ii) the bulk temperature increases as well which in turns (iii) reduces the film thickness. **The observed**  
 18 **link between bulk temperature and scuffing is consistent with literature [32], [33].** In order to  
 19 determine the reason for scuffing initiation a procedure able to isolate one phenomenon is required. As  
 20 the link between dissipated power and bulk temperature is very strong, a new procedure based on  
 21 driving film thickness is needed to investigate its influence.  
 22

# 1 Driving the film thickness: a new experimental procedure

## 2 Test method

3 A widely used model for film thickness (central  $h_c$  or minimal  $h_m$ ) estimation in elliptical contacts is  
4 given by Hamrock and Dowson [30], [31]:

$$5 \quad h_c = 2.69 \times U^{0.67} \times G^{0.53} \times W^{-0.067} \times (1 - 0.61e^{-0.73k}) \times R_x \quad (2)$$

$$6 \quad h_m = 3.63 \times U^{0.68} \times G^{0.49} \times W^{-0.073} \times (1 - e^{-0.68k}) \times R_x \quad (3)$$

7 With

$$8 \quad U = \frac{\eta_{P_{atm}, T_b} v_e}{E' R_x} \quad (4)$$

$$9 \quad G = \alpha E' \quad (5)$$

$$10 \quad W = \frac{F_n}{E' R_x^2} \quad (6)$$

11 According to equation (2), during an experiment on the twin-disk machine where the material and  
12 lubricant are defined, the film thickness is governed by the load  $F_n$ , entrainment speed  $v_e$  and bulk  
13 temperature  $T_b$  of the specimens. As bulk temperature is not a drivable parameter and load has little  
14 influence on film thickness, the proposed procedure focuses on the entrainment speed.

15 The idea of this method is to keep the load and sliding speed (dashed line on Figure 5) constant during  
16 the test while the entrainment speed is gradually decreased (continuous line on Figure 5). Dissipated  
17 power is then only driven by the friction coefficient, which gives us the opportunity to reduce the film  
18 thickness, potentially until scuffing occurs, with minimal friction losses variations (and minimal  
19 temperature variations).

20 If the minimal entrainment speed is reached without scuffing (no sudden friction increase), the first  
21 step performed is repeated to check that the friction coefficient is repeatable and validate that the  
22 surfaces were not altered during the previous steps. The concatenation of these steps constitutes a  
23 block visible on Figure 5.

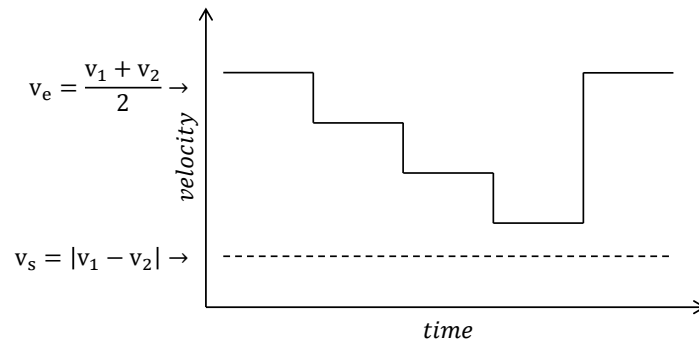


Figure 5: Surface speed parameters during the test block

24 Test blocks are then conducted successively with an increase in sliding speed between each ones  
25 (Figure 6) at constant load and oil injection temperature until a sudden increase in friction, typical of  
26 scuffing, occurs or stopping criteria (maximum sliding speed) is reached. Flow chart of the procedure  
27 is presented in Figure 7. Specimens are then inspected using a 3D optical surface profilometer to  
28 validate the apparition of scuffing.

29

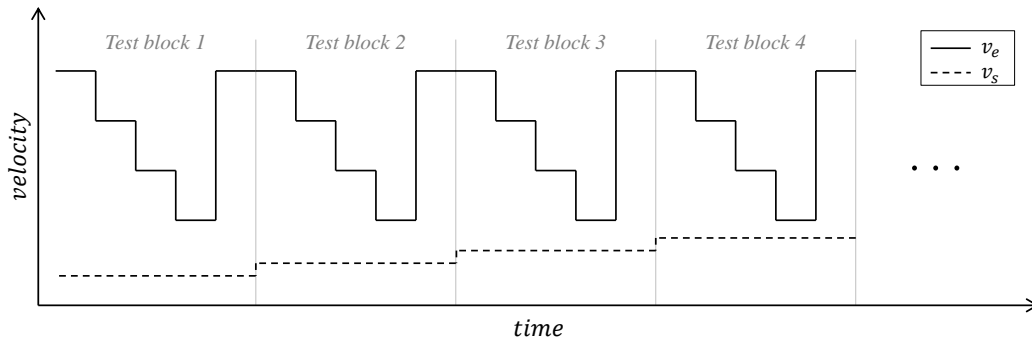


Figure 6: Surface speed parameters during a complete test procedure

1

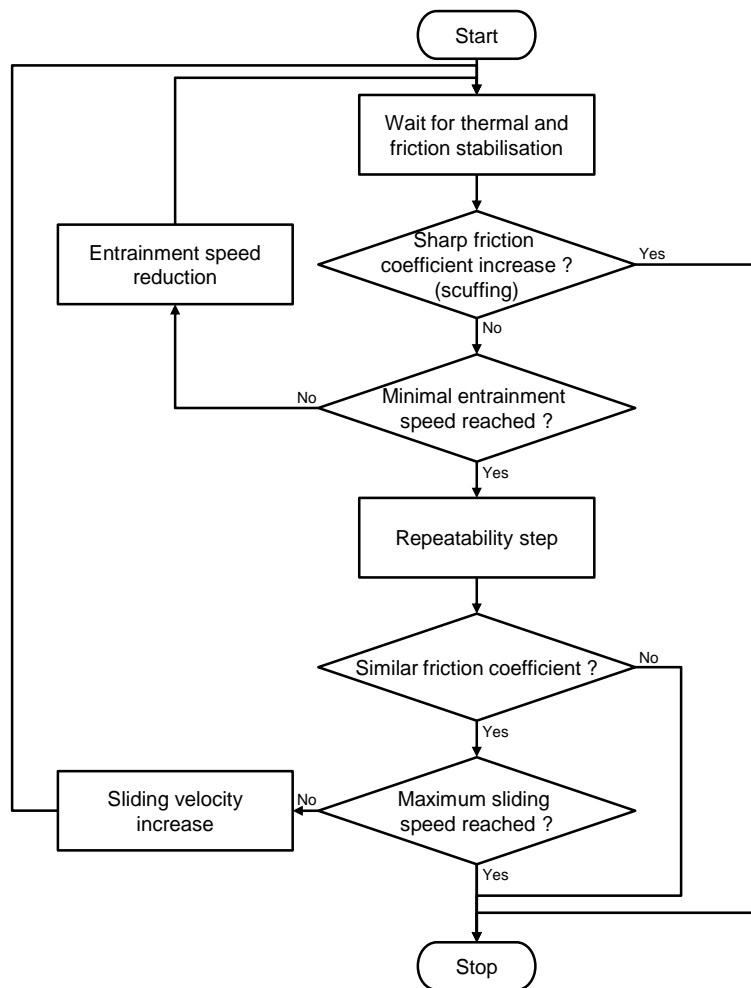


Figure 7: Flow chart describing the test procedure

2

### 3 Experiments

4 A tests was performed on smooth ( $R_a < 0.02 \mu\text{m}$ , typical roughness profile presented on Figure 8)  
 5 nitrided steel disks (see Table 1) with a synthetic base oil (see Table 2). This test will be used to  
 6 analyze the proposed test method regarding the film thickness variations.

7

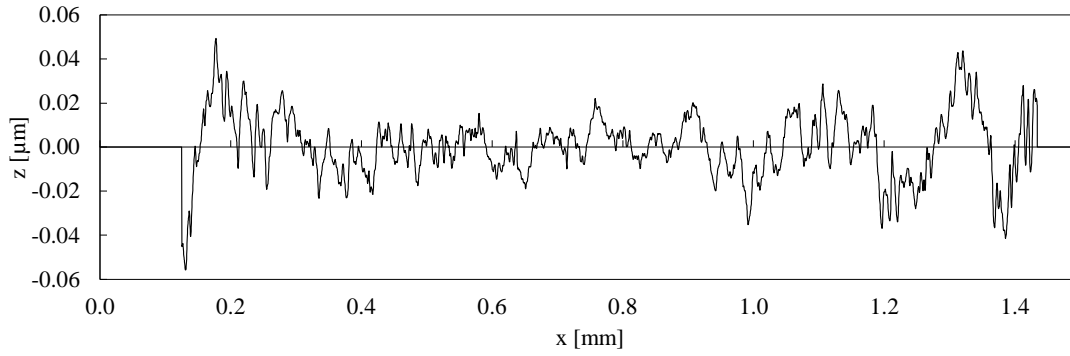


Figure 8: Typical roughness profile obtained on smooth discs, measured in the direction of sliding on disk 1

1

2 Table 1

3 Geometry and surface parameters of the discs

	Symbol	Unit	Disk 1	Disk 2
Radius	$R_x$	m	0.035	0.035
Crown radius	$R_y$	m	$\infty$	0.2
Width	L	m	0.01	0.01
Mean roughness in the direction of sliding	$Ra_s$	$\mu\text{m}$	0.011	0.018
Quadratic roughness in the direction of sliding	$Rq_s$	$\mu\text{m}$	0.014	0.022

4

5 Table 2

6 Oil characteristics

	Symbol	Unit	Value
Kinematic viscosity	$\nu_{40-100}$	cSt	24.5 ; 5.1
Density	$\rho_{15}$	$\text{kg/m}^3$	987
Pressure-viscosity coeff.	$\alpha$	$\text{GPa}^{-1}$	16
Temp.-viscosity coeff.	$\beta$	K	3056

7

8 The test was conducted at a Hertzian maximum contact pressure of 1.6GPa with an oil inlet  
 9 temperature of 100°C. The entrainment speed was decreased from 30 to 10m/s inside a test block and  
 10 the sliding speed ranged from 6 to 10m/s over the test which induced a variation in the friction  
 11 coefficient  $\mu$  from 0.012 to 0.017 (Figure 9). This new procedure induced a variation of the friction  
 12 losses between 263 - 576W over 4 hours (Figure 10). These variations caused the bulk temperature of  
 13 the disks to vary between 120 and 160°C. The duration of each step was set to 10 minutes then  
 14 shortened to 5 minutes as thermal stability on the disks was reached.

15 Friction coefficient did not change during repeatability steps, suggesting that surfaces were not altered  
 16 during the test until scuffing occurred at  $v_s=10\text{m/s}$ ,  $v_e=10\text{m/s}$  (SRR=100%) and a bulk temperature  $T_b$   
 17 of 166°C. The initiation of scuffing caused the friction coefficient increase sharply.



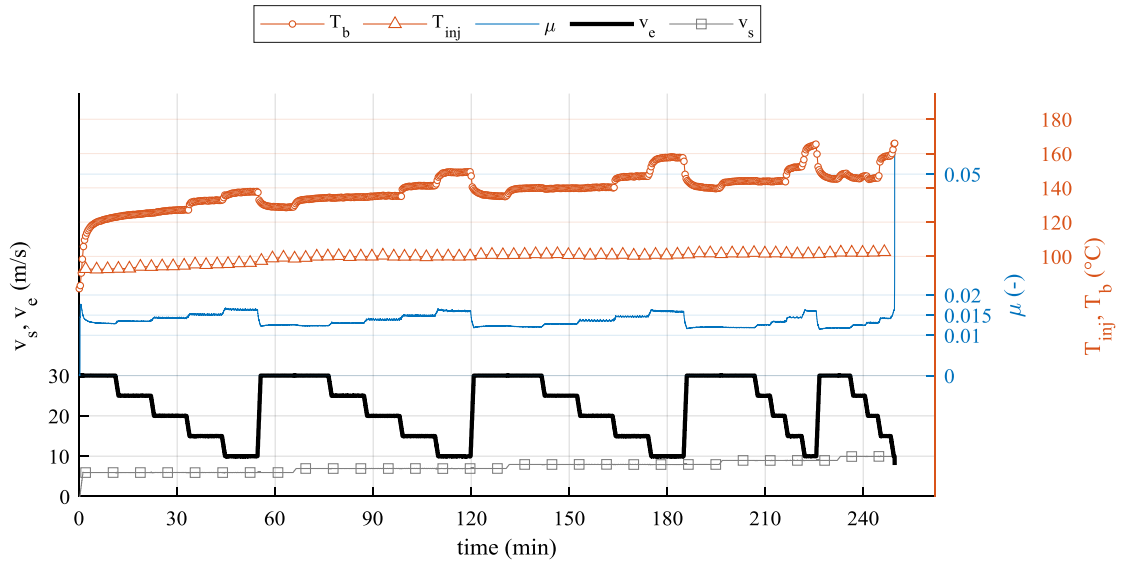


Figure 9: Operating conditions, measured friction coefficient and temperatures for the first test

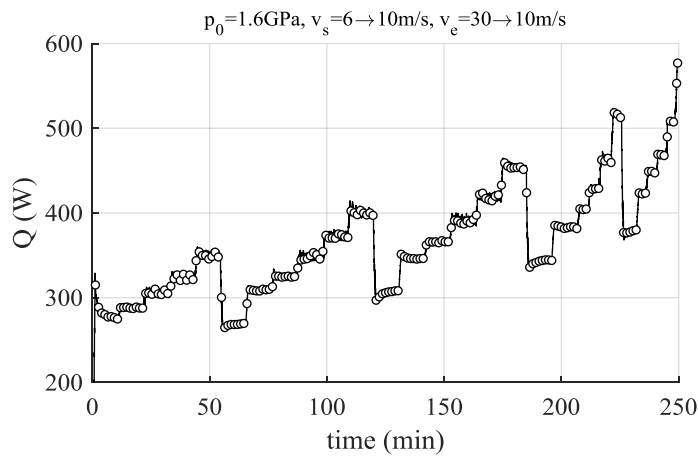


Figure 10: Friction losses during the first test

1  
 2 The surface examination confirmed that scuffing occurred. Scuffing marks can be seen on both  
 3 surfaces and the 3D surface scans (Figure 11, Figure 12) show that material was transferred from the  
 4 slow surface to the fast one. This observation agrees with literature on the direction of material transfer  
 5 when both contacting bodies are made of the same material [23], [24], [34].

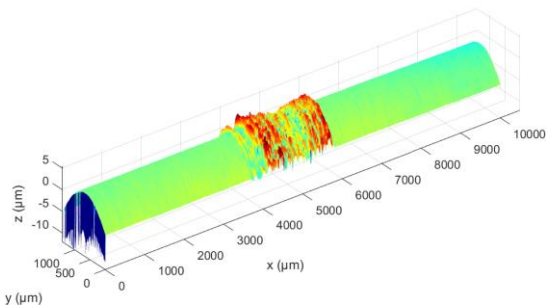


Figure 11: Measured surface, deviation from a disk, fast surface

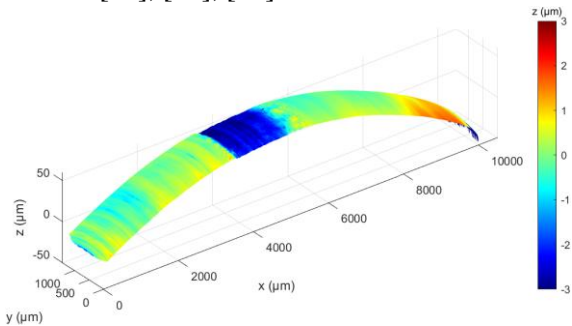


Figure 12: Measured surface, deviation from a crowned disk, slow surface

6  
 7 Using this procedure, in a single experimental test block, the dissipated power is mainly governed by  
 8 friction coefficient. For example, during the third test block (from 130 to 185 minutes), the dissipated

1 power varied from 350 to 450 W (+29%), while in the meantime the film thickness was divided by  
 2 more than two. These variations are visible on Figure 13 and Figure 15. This power variation coupled  
 3 with the heat exchanges between the disks and the environment is responsible for an increase of the  
 4 bulk temperature limited to +18°C (Figure 14). To confirm that the entrainment speed is the main  
 5 influencing parameter on oil film thickness, the influence of this temperature variation is compared to  
 6 the one of the entrainment speed (Figure 15). The minimal film thickness is computed under the  
 7 operating conditions and bulk temperature  $T_b$  measured and compared to the one estimated for a  
 8 constant temperature of 140°C. Then, it appears that the increase in temperature observed during steps  
 9 4 (around  $t = 170\text{min}$ ) and 5 (around  $t = 180\text{min}$ ) is responsible for a relatively small film thickness  
 10 reduction compared to the one induced by the controlled entrainment speed.  
 11 More generally, the contribution of temperature and entrainment speed on film thickness can be  
 12 assessed analytically. Accounting for the load, geometries, material and lubricant used for this test, the  
 13 minimal film thickness equation (3) from Hamrock-Dawson can be reduced as a function of the  
 14 entrainment speed  $v_e$  and bulk temperature  $T_b$  as follow:  
 15

$$h_m(v_e, T_b) = 1.26e^{-8} \times v_e^{0.68} \times e^{\frac{2076.6}{T_b}} \quad (7)$$

16  
 17 The variation of the minimal film thickness  $h_m$  can then be computed within the range of values  
 18 observed during the test for both the entrainment speed and bulk temperature and plotted on Figure 16.  
 19 In this range of temperatures, the controlled variation of the entrainment speed is responsible for a  
 20 variation of the film thickness more than three times greater than the one induced by the temperature  
 21 variations.  
 22 As expected, this procedure allows studying the influence of the film thickness on scuffing by  
 23 controlling it as much as possible on such test rig with minimal power loss and temperature variations.  
 24

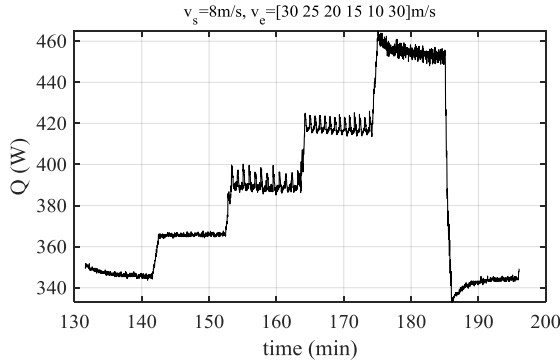


Figure 13: Friction losses during the third test block

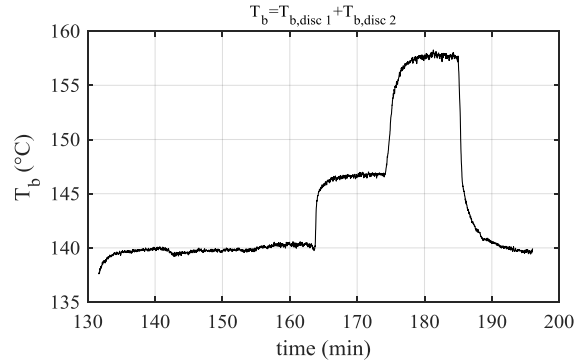


Figure 14: Bulk temperature evolution during the third test block

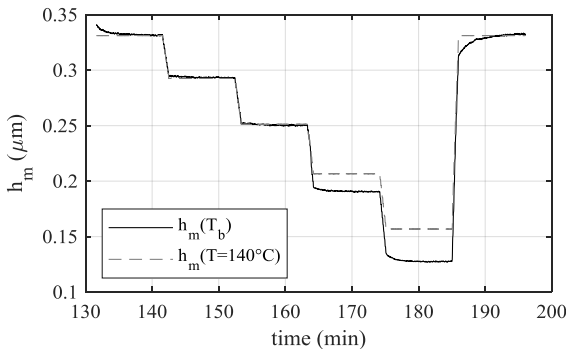


Figure 15: Minimal film thickness variations during the third test block

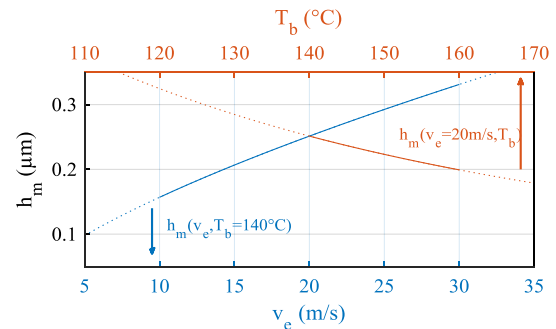
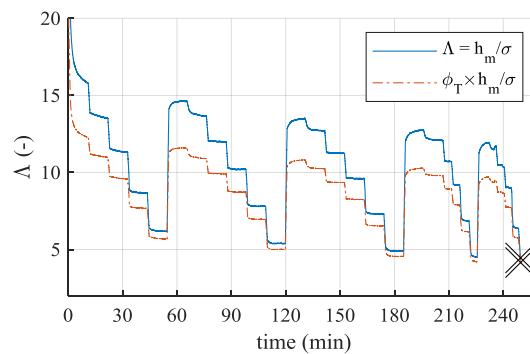


Figure 16: Variation of the film thickness as analytical functions of the temperature and entrainment speed for given operating conditions

1  
 2 According to the film thickness estimated with the Hamrock-Dowson model, and even accounting for  
 3 the thermal reduction factor from Gupta et al. [35], the reduced film thickness  $\Lambda = h_m/\sigma$  (also called  
 4 Tallian parameter) varies during the test (Figure 17) and is minimal ( $\Lambda_{\min}=4.46$ ,  $(\phi_T\Lambda)_{\min}=4.16$ ) at  
 5 scuffing. This high value of the Tallian parameter is a direct consequence of the low magnitude of  
 6 roughness ( $Ra<0.02\mu\text{m}$ ) of the disks used. This parameter is commonly used to describe the  
 7 lubrication regime [36] as follow:

- 8 -  $3 < \Lambda$ : full-film lubrication, the surfaces are fully separated by the oil film
- 9 -  $1 < \Lambda < 3$ : mixed lubrication, the load is supported by the oil film but asperity contact may  
 10 occur
- 11 -  $\Lambda < 1$ : boundary lubrication, a significant part of the load is supported by asperity



12  
 Figure 17: Reduced film thickness evolution during the test

13  
 14 Even though the contact appears to operate under full film lubrication ( $\Lambda>3$ ), scuffing was initiated  
 15 and material was transferred between disks. Assuming the reliability of the models used, only the  
 16 collapse of the oil film could explain the transition from full film lubrication to metal-to-metal contact  
 17 that lead to material transfer.

18 **The proposed test method is based on a theoretical estimation of oil film thicknesses [30], [31]. This**  
 19 **one cannot be measured on the test rig used. These models are validated in the literature ([37]–[39]).**  
 20 **Nevertheless, tests with lubricants of different viscosities, among others, would allow the method to be**  
 21 **generalized.** This new test procedure allowed scuffing initiation through the driving of the film  
 22 thickness. The fact that in usual procedures scuffing is triggered by an increase of load or sliding speed  
 23 shows that scuffing can be achieve in different ways. In order to bring elements of comprehension  
 24 around this complex type of failure the different parameters able to trigger scuffing have to be  
 25 identified.

## 27 Investigation of the bulk temperature

28 The wide spread of the total temperature criteria in the literature suggests that scuffing is a temperature  
 29 induced failure. The total temperature being the addition of the bulk temperature  $T_b$  and the  
 30 temperature rise occurring in the contact [12], [13], scuffing could be achieved through the increase of  
 31 either one of these parameters. In order to investigate this idea, another test has been performed aiming  
 32 to trigger scuffing through the rise of the bulk temperature at constant operating conditions (load,  
 33 sliding and entrainment speeds).

34 The experiment was conducted under the scuffing conditions of normal load, sliding and entrainment  
 35 speeds of the previous test. In order to increase the bulk temperature, the test was started at ambient  
 36 temperature ( $20^\circ\text{C}$ ) and heating of the oil in the injection system was disabled to let the power losses  
 37 drive the temperatures. Specimens of the same geometry, material and surface roughness as in the  
 38 previous test were used. Stable operating conditions in term of sliding speed was reached after 17

1 minutes. The bulk temperature was slowly increasing, for example between 40 and 121 minutes the  
 2 bulk temperature increased from 150 to 157°C, until a sharp increase in friction occurred. Surface  
 3 observation after the test showed visible scuffing marks as underlined in Figure 20b.

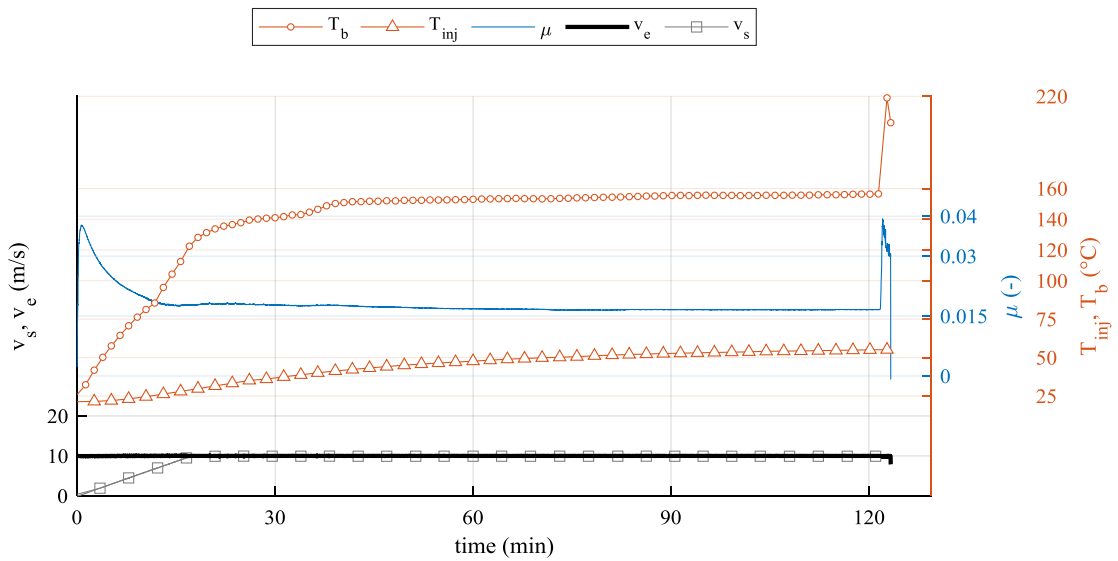


Figure 18: operating conditions, measured friction coefficient and temperatures for the second test

4  
5  
6  
7  
8  
9  
10  
11  
12

As for the first test, the reduced film thickness indicates that the contact is fully lubricated ( $\Lambda_{min}=5.1$ ) until scuffing occurred (Figure 19). The failure initiated at a bulk temperature of 157°C, close to the one of the previous test (166°C). A brown coloration of the track was observed 30 min before scuffing and is shown on Figure 20a. As the contact is fully lubricated, this coloration could be associated to the thermal degradation of oil in the contact. This suggests that the test performed on the edge of scuffing for a long period (more than 1 hour) until the temperature became sufficient to cause the total collapse of the film. These brown oil marks were replaced by scuffing marks visible on Figure 20b.

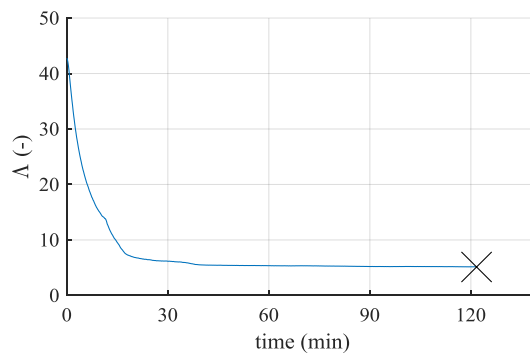


Figure 19: Reduced film thickness for the second test

13

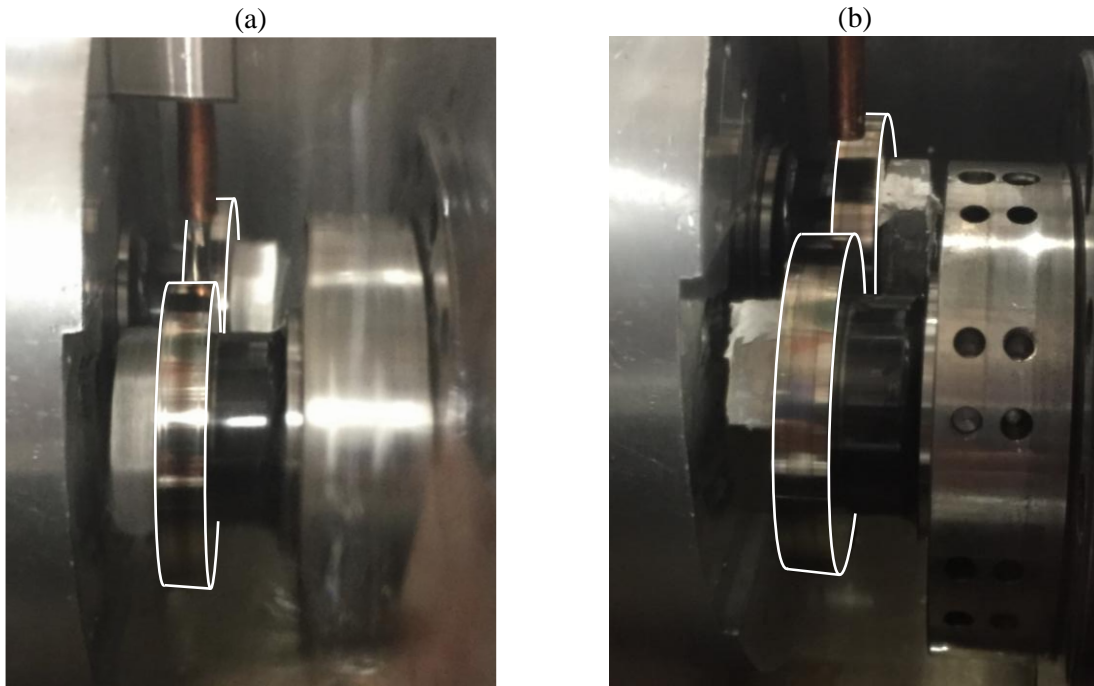


Figure 20: Photographs of the discs (a) 30 min before scuffing and (b) after scuffing, contours of the discs have been redrawn for visibility

1  
2  
3  
4  
5  
6  
7  
8  
9  
10  
11  
12  
13  
14  
15  
16

From the information gathered in literature and during tests, a mechanism for scuffing can be proposed for a given contact. The environment (operating conditions, lubrication) drives the bulk temperature, which then influences the lubricant film thickness through changes in viscosity. This in turns influences the lubricant and asperities shearing, which generates friction losses that drives the bulk temperature. This looped multiscale mechanism (represented on Figure 21) may lead to stable operating or sudden failure of the contact through scuffing, which affects the entire system efficiency.

Different procedures have been investigated to develop scuffing while focusing on different parameters: dissipated power, oil film and bulk temperature. These different test methods for scuffing study are represented in green on Figure 21.

Although the particular link in this scuffing circle leading to the failure is not yet well identified, one exit point can be identified from the tests performed: the collapse of the oil film in full film lubrication (represented in orange on Figure 21). The variety of parameters able to influence scuffing may be the reason for which the literature does not agree on a criterion, and drives to search for a combination of parameters.

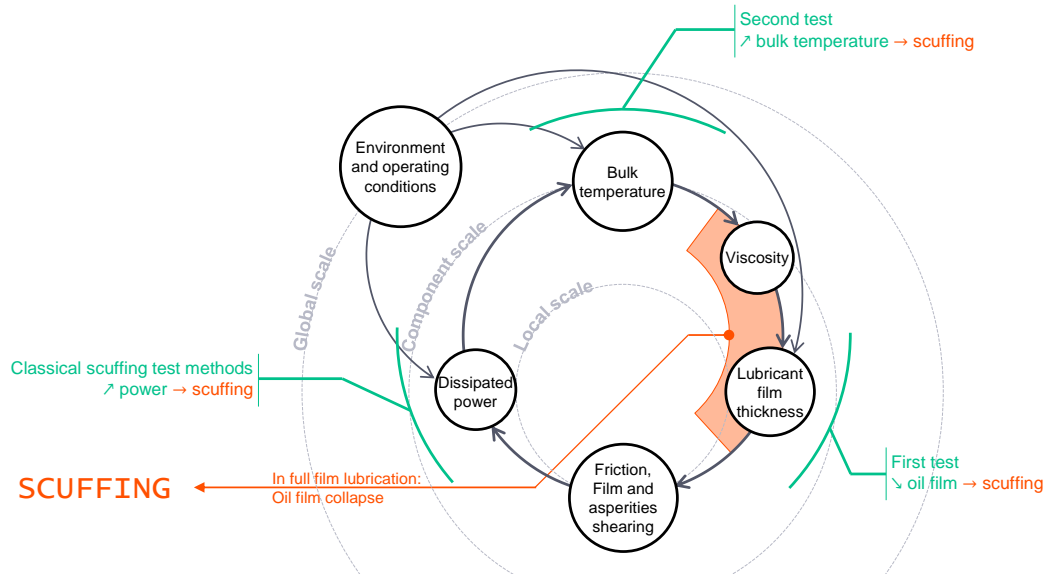


Figure 21: Multiscale approach for scuffing

## 1 Conclusion

2 A traction test procedure for scuffing has been investigated in detail. Strongly coupled parameters  
 3 (friction power losses, temperature and oil film thickness) have been identified, along with the  
 4 relations they follow. These mechanisms can be found in usual test procedures used for scuffing  
 5 investigations, and may increase the difficulty to understand scuffing phenomena.

6 Typical experimental studies of scuffing are based on measurements and analyses of dissipated power  
 7 or on temperature considerations. A new experimental procedure for scuffing study on a twin disk  
 8 machine allowing the film thickness to be controlled, is presented. The film thickness is calculated  
 9 using the well-known Hamrock Dowson formula from the measured parameters (normal load, speeds,  
 10 and oil and steel characteristics). The oil film thickness seems to be a key parameter to study scuffing  
 11 initiation.

12 Furthermore, the variety of operating conditions encountered before reaching scuffing is larger than  
 13 regular procedures. This test procedure might be a powerful tool to gather data on scuffing and might  
 14 be complementary with usual faster procedures once the mechanism of scuffing is understood.

15 Although asperity contact is commonly regarded as necessary for scuffing initiation, it was achieved  
 16 in full film lubrication using base oil and smooth surfaces.

17 Additional test demonstrated that scuffing could also be triggered by the rising bulk temperature. A  
 18 scuffing circle highlighting the strong couplings between influential parameters has been presented.  
 19 The three test methods discussed in this paper allow driving different parameters in order to reach  
 20 scuffing. A first exit point from this scuffing circle has been drawn from the tests performed. In the  
 21 case of full film lubrication, the oil film is susceptible to collapse under severe operating conditions,  
 22 causing metal-to-metal contact leading to the material transfer typical of scuffing.

23 All tests were performed using nitrided steel and a synthetic base oil. The use of different materials  
 24 and lubricants will allow the accuracy of the proposed method to be evaluated under various  
 25 conditions. This will be a necessary step in understanding initiation mechanisms of scuffing.

26

## 27 Declaration of Conflicting Interests

28 The author(s) declared no potential conflicts of interest with respect to the research, authorship, and/or  
 29 publication of this article.

30

## 1 Funding

2 The author(s) disclosed receipt of the following financial support for the research, authorship, and/or  
3 publication of this article: The authors would like to thank SAFRAN Transmission Systems for  
4 funding this research and ANRT for their financial support.

## 5 References

- 6 [1] A. Dyson, "Scuffing - a review," *Tribol. Int.*, vol. 8, no. 2, pp. 77–87, 1975.
- 7 [2] A. Dyson, "Scuffing - a review. Part 2: The mechanism of scuffing," *Tribology International*,  
8 vol. 8, no. 3. 1975.
- 9 [3] J. Grosberg, "A critical review of gear scoring criteria," *Wear*, vol. 43, no. 1, 1977.
- 10 [4] W. F. Bowman and G. W. Stachowiak, "A review of scuffing models," *Tribol. Lett.*, vol. 2, no.  
11 2, pp. 113–131, 1996.
- 12 [5] K. C. Ludema, "A review of scuffing and running-in of lubricated surfaces, with asperities and  
13 oxides in perspective," *Wear*, vol. 100, no. 1–3, 1984.
- 14 [6] J. Castro and J. Seabra, "Scuffing and lubricant film breakdown in FZG gears part I. Analytical  
15 and experimental approach," *Wear*, vol. 215, no. 1–2, pp. 104–113, 1998.
- 16 [7] J. O. Almen, "Dimensional value of lubricants in gear-design," in *SAE Technical Papers*, 1942.
- 17 [8] J. O. Almen, "Factors influencing the durability of spiral bevel gears for automobiles," *Autom.*  
18 *Ind.*, vol. 73, p. 662, 1935.
- 19 [9] J. O. Almen, "Surface deterioration of gear teeth," *Mech. Wear*, vol. 229, 1950.
- 20 [10] R. M. Matveevsky, "The critical temperature of oil with point and line contact machines," *J.*  
21 *Fluids Eng. Trans. ASME*, vol. 87, no. 3, 1965.
- 22 [11] R. M. Matveevsky, "Friction power as a criterion of seizure with sliding lubricated contact,"  
23 *Wear*, vol. 155, no. 1, 1992.
- 24 [12] H. Blok, "The flash temperature concept," *Wear*, 1963.
- 25 [13] H. Blok, "The postulate about the constancy of scoring temperature," *Interdiscip. approach to*  
26 *Lubr. Conc. contacts*, pp. 153–248, 1969.
- 27 [14] Y. S. Muzychka and M. M. Yovanovich, "Thermal resistance models for non-circular moving  
28 heat sources on a half space," *J. Heat Transfer*, vol. 123, no. 4, 2001.
- 29 [15] H. Christensen, "Failure by collapse of hydrodynamic oil films," *Wear*, vol. 22, no. 3, 1972.
- 30 [16] M. Cocks and T. E. Tallian, "Sliding contacts in rolling bearings," *ASLE Trans.*, vol. 14, no. 1,  
31 1971.
- 32 [17] T. E. Tallian, "The theory of partial elastohydrodynamic contacts," *Wear*, vol. 21, no. 1, 1972.
- 33 [18] J. Castro and J. Seabra, "Global and local analysis of gear scuffing tests using a mixed film  
34 lubrication model," *Tribol. Int.*, vol. 41, no. 4, pp. 244–255, Apr. 2008.
- 35 [19] C. Hangan, I. C. Romanu, and I. Muscă, "About four balls scuffing test parameters," in *IOP*  
36 *Conference Series: Materials Science and Engineering*, 2020, vol. 997, no. 1.
- 37 [20] W. Piekoszewski, M. Szczerek, and W. Tuszynski, "The action of lubricants under extreme  
38 pressure conditions in a modified," *Wear*, vol. 249, no. 3–4, pp. 188–193, 2001.
- 39 [21] S. Li, "Influence of surface roughness lay directionality on scuffing failure of lubricated point  
40 contacts," *J. Tribol.*, vol. 135, no. 4, 2013.
- 41 [22] S. Li, A. Kahraman, N. E. Anderson, and L. D. Wedeven, "A model to predict scuffing failures  
42 of a ball-on-disk contact," *Tribol. Int.*, vol. 60, pp. 233–245, 2013.
- 43 [23] G. Isaac, C. Chagnenet, F. Ville, J. Cavoret, and S. Becquerelle, "Thermal analysis of twin-disc  
44 machine for traction tests and scuffing experiments," *Proc. Inst. Mech. Eng. Part J J. Eng.*  
45 *Tribol.*, vol. 232, no. 12, pp. 1548–1560, 2018.
- 46 [24] D. Nélias, "Étude expérimentale et théorique du microgrippage dans les contacts  
47 élastohydrodynamiques," *Rev. Gen. Therm.*, 1997.
- 48 [25] M. J. Handschuh, A. Kahraman, and N. E. Anderson, "Development of a High-Speed Two-  
49 Disk Tribometer for Evaluation of Traction and Scuffing of Lubricated Contacts," *Tribol.*  
50 *Trans.*, pp. 1–26, Jan. 2020.
- 51 [26] J. Castro and J. Seabra, "Scuffing and lubricant film breakdown in FZG gears part II. New PV  
52 scuffing criteria, lubricant and temperature dependent," *Wear*, vol. 215, no. 1–2, pp. 114–122,

1 1998.

2 [27] P. Navet, C. Changenet, F. Ville, D. Ghribi, and J. Cavoret, “Thermal Modeling of the FZG

3 Test Rig: Application to Starved Lubrication Conditions,” *Tribol. Trans.*, 2020.

4 [28] M. J. Handschuh, S. Li, A. Kahraman, and D. Talbot, “An Experimental–Theoretical

5 Methodology to Develop Scuffing Limits for Relatively Smooth High-Speed Contacts,” *Tribol.*

6 *Trans.*, vol. 63, no. 5, 2020.

7 [29] F. Ville, D. Nélias, G. Tournonias, L. Flamand, and P. Sainsot, “On the two-disc machine: A

8 polyvalent and powerful tool to study fundamental and industrial problems related to

9 elastohydrodynamic lubrication,” in *Tribology Series*, 2001, vol. 39, pp. 393–402.

10 [30] B. J. Hamrock and D. Dowson, “Isothermal Elastohydrodynamic Lubrication of Point

11 Contacts: Part III-Fully Flooded Result,” *J. Tribol.*, vol. 99, no. 2, 1977.

12 [31] D. Brewe and B. J. Hamrock, “Simplified solution for elliptical-contact deformation between

13 two elastic solids,” *J. Tribol.*, vol. 99, no. 4, 1977.

14 [32] S. Li and A. Kahraman, “A scuffing model for spur gear contacts,” *Mech. Mach. Theory*, vol.

15 156, 2021.

16 [33] B. R. Höhn and K. Michaelis, “Influence of oil temperature on gear failures,” *Tribol. Int.*, vol.

17 37, pp. 103–109, 2004.

18 [34] H. Blok and Others, “Les températures de surface dans des conditions de graissage sous

19 extrême pression,” in *2nd World Petroleum Congress*, 1937.

20 [35] P. K. Gupta, H. S. Cheng, D. Zhu, N. H. Forster, and J. B. Schrand, “Viscoelastic effects in

21 MIL-L-7808-type lubricant, part I: Analytical formulation,” *Tribol. Trans.*, vol. 35, no. 2, pp.

22 269–274, 1992.

23 [36] P. Guay, “Principes de base la lubrification,” *Tech. l’Ingénieur*, vol. tri1500, 2014.

24 [37] D. Jalali-Vahid, H. Rahnejat, R. Gohar, and Z. M. Jin, “Comparison between experiments and

25 numerical solutions for isothermal elastohydrodynamic point contacts,” *Journal of Physics D:*

26 *Applied Physics*, vol. 31, no. 20. 1998.

27 [38] R. Kumar, M. S. Azam, S. K. Ghosh, and S. Yadav, “70 years of Elastohydrodynamic

28 Lubrication (EHL): A Review on Experimental Techniques for Film Thickness and Pressure

29 Measurement,” *Mapan - Journal of Metrology Society of India*, vol. 33, no. 4. Springer, pp.

30 481–491, 01-Dec-2018.

31 [39] K. A. Keys and W. O. Winer, “An experimental evaluation of the Hamrock and Dowson

32 minimum film thickness equation for fully flooded ehd point contacts,” *J. Tribol.*, vol. 103, no.

33 2, pp. 284–294, 1981.

34

35

36



# 1 Appendix

## 2 Roman letters

$E'$	Pa	reduced elastic modulus ( $=2/\left(\frac{1-\nu_1^2}{E_1} + \frac{1-\nu_2^2}{E_2}\right)$ )
$F_n$	N	normal load
$h_c$	m	central film thickness
$h_m$	m	minimal film thickness
$k$	–	ellipticity ratio ( $=1.0339\left(\frac{R_y}{R_x}\right)^{0.636}$ )
$L$	m	width of the disk
$p_0$	Pa	Hertz contact pressure
$Q$	W	friction losses ( $=\mu F_n v_s$ )
$Ra_s$	m	arithmetic roughness in the direction of sliding
$Rq_s$	m	quadratic roughness in the direction of sliding
$R_x$	m	equivalent rolling radius ( $=1/(1/R_{x1} + 1/R_{x2})$ )
$R_y$	m	crown radius
$T_b$	°C	bulk temperature
$T_{oil}$	°C	oil injection temperature
$v_1$	m. s <sup>-1</sup>	rolling speed of surface 1
$v_2$	m. s <sup>-1</sup>	rolling speed of surface 2
$v_e$	m. s <sup>-1</sup>	entrainment speed ( $=(v_1+v_2)/2$ )
$v_r$	m. s <sup>-1</sup>	rolling speed speed ( $=v_1+v_2$ )
$v_s$	m. s <sup>-1</sup>	sliding speed ( $=v_1-v_2$ )

3

## 4 Greek letters

$\alpha$	Pa <sup>-1</sup>	pressure-viscosity coefficient
$\beta$	K	temperature-viscosity coefficient
$\nu_{40}$	cSt	absolute oil kinematic viscosity at 40°C
$\nu_{100}$	cSt	absolute oil kinematic viscosity at 100°C
$\Lambda$	–	reduced film thickness
$\mu$	–	friction coefficient
$\Phi_T$	–	thermal reduction factor
$\eta_{p_{atm}, T_b}$	Pa. s	oil dynamic viscosity at ambient pressure and bulk temperature
$\rho$	kg. m <sup>-3</sup>	oil density
$\sigma$	m	RMS of quadratic roughness ( $=\sqrt{Rq_{1,s}^2 + Rq_{2,s}^2}$ )

5

## 6 Abbreviations

FP	–	Friction Power / friction losses
FPI	–	Friction Power Intensity
PV	–	Pressure Velocity
SRR	%	slide-to-roll ratio ( $=v_s/v_e$ )

7